Life-Cycle and Sustainability of Civil Infrastructure Systems – Strauss, Frangopol & Bergmeister (Eds)
 ISBN 978-0-415-62126-7

Prediction of fatigue damage accumulation in metallic structures by the estimation of strains from operational vibrations

C. Papadimitriou
University of Thessaly, Volos, Greece

E.-M. Lourens, G. Lombaert, G. De Roeck & K. Liu
K. U. Leuven, Leuven, Belgium

ABSTRACT: This work deals with the problem of estimating damage accumulation due to fatigue in the entire body of a metallic structure using operational vibration measurements collected from a limited number of sensors installed on a structure. A recently proposed joint input-state estimation filter is extended to estimate the strain response time histories in the entire body of the structure using the output-only vibration measurements. The estimates hold for any excitation with arbitrary temporal variation and spatial distribution over the structure. Such predictions are then integrated with damage accumulation models, S-N fatigue curves and rainflow stress cycle counting methods to estimate fatigue damage accumulation maps covering the entire body of the structure. The method is validated using simulated vibration measurements for a laboratory steel beam, generated from impulse and stochastic excitations.

1 INTRODUCTION

During operation of a structure, output-only response measurements can be conveniently recorded using a permanently installed network of sensors. Such vibration measurements are widely used to estimate the modal characteristics of the structure (Reynders and De Roeck 2008), to update finite element models (Mottershead & Friswell 1993), to identify the location and severity of damage (e.g. Ntotsios et al. 2009, Teughels & De Roeck 2005), to identify the temporal and spatial variation of the loads applied on the structure (Lourens et al. 2012a), to estimate the state (Ching et al. 2007, Wu & Smyth 2007, Hernandez and Bernal 2008, Chatzi & Smyth 2009), as well as to update robust predictions of system performance (Papadimitriou et al. 2001). In particular, among the various uses of the state estimates based on output-only vibration measurements, an important one that only recently received special attention is the prediction of the fatigue damage accumulation in metallic components of structures (Papadimitriou et al. 2011).

Damage accumulation due to fatigue is an important safety-related issue in metallic structures. Information on fatigue damage accumulation is valuable for structural risk assessment and for designing optimal, cost-effective inspection / maintenance strategies. Fatigue damage accumulation at critical points of a structure can be estimated using available damage accumulation models that analyze the actual stress time histories developed during operation (Palmgren 1924, Miner 1945). However, inferring the stress time histories in a structure under actual operational conditions using strain rosettes has severe limitations since the number of sensors is limited and, therefore, the sensor network cannot cover the entire structure or all critical structural locations. The characteristics of the stress response time histories at a point in a structure can alternatively be predicted by using a model of the structure (e.g. a finite element model) and the actual excitation time histories. However, for most structures, the excitation time histories during operation are neither available nor can they be conveniently measured by a network of sensors.

Predictions of the strain time histories in a large number of unmeasured critical locations can be possible if one combines the available output-only measurements with the information obtained from a finite element model of the structure. This is a challenging problem that is currently under investigation with promising solutions proposed recently (Lourens et al. 2012a and 2012b). Such estimates are crucial for producing complete fatigue damage accumulation maps based on the actual operational conditions and not on statistical models that have been derived by processing data from a group of structures, failing to be representative of the actual condition in a member of the group.

These developments are very important for planning cost-effective maintenance strategies of number of structures that take into account the actual condition of the structure instead of being based on statistical models derived from data from a group of structures.

The work by Papadimitriou et al. (2011) was a first attempt along this direction. Prediction of fatigue accumulation was based solely on the spectral characteristics of the strain time histories, assuming that the time histories can be considered stationary over short enough time intervals. Specifically, the fatigue damage accumulation in critical locations of the entire structure was obtained by integrating (a) methods for predicting strain/stress response time histories and their correlation/spectral characteristics in the entire structure from output-only measured response time histories available at limited locations in the structure, and (b) frequency domain methods (Lutes & Larsen 1990) for estimating fatigue damage accumulation using the spectral characteristics of the predicted strain/stress response time histories. In particular, Kalman filter methods were used to predict the spectral characteristics of the strain/stress response time history at various locations within structural components using measurements available at a limited number of locations. The main assumption was that the excitation or portions of the excitations can be approximated by a stationary stochastic process.

For a number of applications, however, the assumption of stationarity is either violated or is not representative of the actual excitation conditions. An obvious case in civil engineering where the non-stationarity of the excitation and response is pronounced includes the passage of trains or heavy trucks over metallic bridges. The fatigue under train or large truck loads is an important safety issue. However, the damage accumulation predictions proposed in Papadimitriou et al. (2011) are not applicable. Consequently, there is a need to develop new estimation methods capable of predicting the full strain response time histories that will be more appropriate in case of non-stationary excitations.

This work deals with the problem of estimating the full strain time histories at critical locations of the structure using operational vibration measurements from a limited number of sensors and the use of such estimates to predict fatigue damage accumulation in the entire body of a metallic structure. No assumptions are made on the spatial and temporal characteristics of the applied loads, as in Papadimitriou et al. (2011). For this purpose, a joint input-state estimation filter proposed in Lourens et al. (2012b) is adopted and extended to estimate strain response time histories in the entire body of the structure using output-only vibration measurements collected from the sensor network. The proposed methodology is validated using simulated data from a laboratory beam structure subjected to impulse-type and stochastic excitations.

2 FATIGUE DAMAGE ACCUMULATION FROM OPERATIONAL VIBRATIONS

2.1 *General considerations*

Predictions of fatigue damage accumulation at a point in a structure are often based on models that consider the stress response time histories at that point. Such stress response time histories can be readily inferred from strain response time histories directly measured using strain rosettes attached to the structure. However, such predictions are only applicable for the locations where measurements are available. A large number of strain sensors is therefore required to cover all hot spot locations in large structures in civil engineering and related applications. Due to practical and economical considerations, the number of sensors placed in a structure during operation is very limited and in most cases does not allow covering all critical locations. Moreover, at some locations in the structures sensors cannot be installed, e.g. underwater locations for fully submerged structures and offshore structures (oil refinery structures, offshore wind turbines, offshore steel jackets, etc.), and in-accessible areas of large structures.

To proceed with fatigue predictions one has to infer the strain response time histories based on the information contained in measurements from the system of sensors attached to the structure. Such predictions are possible if one combines the information in the measurements with information obtained from a model (e.g. a finite element model) of the structure. It is important to note that such estimations will reflect the actual strain time histories developed on the structure during operation and thus the corresponding fatigue damage accumulation estimates will be representative of the actual fatigue accumulated in the structure at the point under consideration. Repeating such estimates at all points in the structure, one is able to develop realistic fatigue damage accumulation maps that cover the entire structure.

The fatigue damage accumulation in the entire structure thus involves integration of (a) methods for estimating strain response time histories from the information contained in a limited number of sensors, and (b) fatigue damage accumulation models. The analyses in this study are restricted to the case of linear structures and stress response predictions at locations subjected to uni-axial stress states. Without loss of generality, the measured quantities are considered to be accelerations.

The fatigue damage accumulation method is described next. The method for estimating the strain response time history using operational vibration measurements is presented in Section 3.

2.2 *Fatigue damage accumulation*

The Palmgren -Miner rule (Palmgren 1924, Miner 1945) is commonly used to predict the damage accumulation due to fatigue. According to this rule, a linear damage accumulation law at a point in the structure subjected to variable amplitude stress time history is defined by the formula

$$D=\sum_{i}^{k}\frac{n_i}{N_i} \tag{1}$$

where n_i is the number of cycles at a stress level σ_i, N_i is the number of cycles required for failure at a stress level σ_i, and k is the number of stress levels identified in a stress time history at the corresponding structural point.

S-N fatigue curves available from laboratory experiments on simple specimens subjected to constant amplitude loads, are used to describe the number of cycles N_i required for failure in terms of the stress level σ_i. The number of cycles n_i at a stress level σ_i is usually obtained by applying stress cycle counting methods on the stress time histories measured or estimated for the point under consideration. Herein, the rainflow cycle-counting method is used (ASTM E-1049 1997). The fatigue accumulation model is revised to account for a non-zero mean stress according to the Goodman relationship (Tunna 1986):

$$\Delta\sigma_{\mathrm{Rt}}=\Delta\sigma_{\mathrm{R}}\left(1-\frac{\sigma_{\mathrm{m}}}{\sigma_{\mathrm{u}}}\right) \tag{2}$$

where $\Delta\sigma_{\mathrm{Rt}}$ is the modified stress cycle range, $\Delta\sigma_{\mathrm{R}}$ is the original stress cycle range, σ_{m} is the mean stress, and σ_{u} is the static strength of the material.

Applying Miner's rule, the fatigue damage of a structural detail depends on the stress range spectrum (stress range $\Delta\sigma$ and number of stress cycles n) and the fatigue detail category classified in the Eurocode 3 (EN 1993-1-9 Eurocode 3, 2005) as follows:

$$D=\underbrace{\sum_{j=1}^{k_1}\frac{n_i}{5\times 10^6}\left(\frac{\Delta\sigma_i}{\Delta\sigma_D}\right)^m}_{\Delta\sigma_i\geq\Delta\sigma_D}+\underbrace{\sum_{j=1}^{k_2}\frac{n_j}{5\times 10^6}\left(\frac{\Delta\sigma_j}{\Delta\sigma_D}\right)^{m+2}}_{\Delta\sigma_L\leq\Delta\sigma_j\leq\Delta\sigma_D} \tag{3}$$

where $\Delta\sigma_D$ is the constant amplitude fatigue limit at 5×10^6 cycles; $\Delta\sigma_L$ is the cut-off limit; $\Delta\sigma_i$ and $\Delta\sigma_j$ are the ith and jth stress ranges, n_i and n_j are the number of cycles in each $\Delta\sigma_i$ and $\Delta\sigma_j$ block, and k_1 and k_2 represent the number of different stress range blocks above or below the constant amplitude fatigue limit $\Delta\sigma_D$.

In Eurocode 3, each fatigue detail category is designated by a number which represents, in N/mm^2, the reference value $\Delta\sigma_C$ for the fatigue strength at 2 million cycles. As this study focuses on the accuracy of the fatigue damage predicted by the proposed method, the fatigue detail category 36 is adopted to illustrate the method. The following values of the parameters of the design S-N curves are recommended by Eurocode for detail category 36: $m=3$, $\Delta\sigma_D=26.5$ MPa and $\Delta\sigma_L=14.5$.

3 PREDICTION OF STRAIN TIME HISTORIES FROM OPERATIONAL VIBRATIONS

The objective of this section is to predict the strain response at all points in a structure using measurements at a limited number of locations. This is achieved using an approach that is outlined in this subsection and based on a filter that has the structure of the Kalman filter, but is used to jointly estimate the inputs and the full state of a linear system using a limited number of vibration measurements (Lourens et al 2012b). The filter, which extends Gillijns and De Moor's (2007a and 2007b) joint input-state estimation algorithm to handle structural dynamics applications, was demonstrated to be accurate for estimating acceleration time histories at unmeasured locations in the structure. For displacement and strain time histories, the filter estimates were inaccurate due to low frequency shift manifested in the time histories. Such inaccuracies are corrected in this work by applying a high frequency filter to the estimates provided by the joint input-state estimation filter technique. The main steps of the joint input-state estimation algorithm, first presented in Lourens et al. (2012b), are outlined next.

3.1 *Equations of Motion and Continuous-Time State Space Formulation*

Consider the dynamic response of a linear structural system subjected to a number of excitations. The equations of motion are given by the following set of N second-order differential equations resulting from a spatial discretization of the structure, e.g. by finite element analysis

$$M\underline{\ddot{u}}(t)+C\underline{\dot{u}}(t)+K\underline{u}(t)=S\underline{p}(t) \tag{4}$$

where $\underline{u}(t)\in\mathbb{R}^{N\times1}$ is the displacement vector, M, C and $K\in\mathbb{R}^{N\times N}$ are respectively the mass, damping and stiffness matrices, $\underline{p}(t)\in\mathbb{R}^{N_{in}\times1}$ is the applied excitation vector, and $S\in\mathbb{R}^{N\times N_{in}}$ is a matrix comprised of zeros and ones that maps the N_{in} excitation loads to the N output DOFs. Throughout the analysis, it is assumed that the system matrices M, C and K are symmetric. Let $\underline{y}(t)\in\mathbb{R}^{N_{meas}\times1}$ be the vector that collects all measurements at different locations of the structure at time t. These measurements are expressed in terms of the displacement/strain, velocity and acceleration vectors as

$$\underline{y}(t)=S_a\underline{\ddot{u}}(t)+S_v\underline{\dot{u}}(t)+S_d\underline{u}(t) \tag{5}$$

where S_a, S_v and $S_d \in \mathbb{R}^{N_{meas}\times N}$ are selection matrices for accelerations, velocities and displacements/strains, respectively. These measurements are generally collected from sensors such as accelerometers, strain gauges, etc.

Introducing the state vector $x^T = [u^T, \dot{u}^T] \in \mathbb{R}^{1\times 2N}$, the equation of motion can be written in the state space form

$$\underline{\dot{x}} = A_c \underline{x} + B_c \underline{u}(t) \tag{6}$$

while the measured output vector $\underline{y}(t)$ is given by the observation equation

$$\underline{y}(t) = G_c \underline{x} + J_c \underline{u}(t) \tag{7}$$

where

$$A_c = \begin{bmatrix} 0 & I \\ -M^{-1}K & -M^{-1}C \end{bmatrix} \in \mathbb{R}^{2N\times 2N} \tag{8}$$

is the state transition matrix,

$$B_c = \begin{bmatrix} 0 \\ M^{-1}S \end{bmatrix} \in \mathbb{R}^{2N\times N_{in}} \tag{9}$$

$$G_c = [S_d - S_a M^{-1}K \quad S_v - S_a M^{-1}C] \in \mathbb{R}^{N_{meas}\times 2N} \tag{10}$$

is the output influence matrix, and

$$J = S_a M^{-1} S_p \in \mathbb{R}^{N_{meas}\times 2N_{in}} \tag{11}$$

is the direct transmission matrix.

Assuming that the structure is classically damped, and introducing the coordinate transformation $\underline{u}(t) = \Phi\underline{\xi}(t)$, the modal coordinate vector $\underline{\xi}(t) \in \mathbb{R}^{m\times 1}$, the modeshape matrix $\Phi \in \mathbb{R}^{N\times m}$ and the diagonal matrix $\Omega^2 = diag(\omega_r^2) \in \mathbb{R}^{m\times m}$ of the eigenvalues w_r^2, satisfying $K\Phi = M\Phi\Lambda$, the state vector $\underline{x} \in \mathbb{R}^{2N}$ is given in terms of the modal state vector $\underline{z}^T = [\underline{\xi}^T \quad \underline{\dot{\xi}}^T] \in \mathbb{R}^{1\times 2N}$ in the form

$$\underline{x} = \begin{bmatrix} \Phi & 0 \\ 0 & \Phi \end{bmatrix} \underline{z} \in \mathbb{R}^{2N\times 2N} \tag{12}$$

where the modal state vector $\underline{z}$ and the measurement vector $y(t)$ satisfy equations (6) and (7), respectively, with

$$A_c = \begin{bmatrix} 0 & I \\ -\Omega^2 & -\Gamma \end{bmatrix} \in \mathbb{R}^{2N\times 2N} \tag{13}$$

$$B_c = \begin{bmatrix} 0 \\ \Phi^{-1}S \end{bmatrix} \in \mathbb{R}^{2N\times N_{in}} \tag{14}$$

$$G_c = [S_d\Phi - S_a\Phi\Omega^2 \quad S_v\Phi - S_a\Phi\Gamma] \in \mathbb{R}^{N_{meas}\times 2N} \tag{15}$$

$$J = S_a \Phi\Phi^T S_p \in \mathbb{R}^{N_{meas}\times 2N_{in}} \tag{16}$$

$\Gamma = diag(2\zeta_r w_r) \in \mathbb{R}^{m\times m}$ and ζ_r is the damping ration of the r mode.

3.2 *Discrete-Time State Space Formulation*

Using the sampling rate $1/\Delta t$, the discrete-time state space model corresponding to (6) and (7) is

$$\underline{x}_{k+1} = A\underline{x}_k + B\underline{p}_k + \underline{w}_k \tag{17}$$

$$\underline{y}_k = G\underline{x}_k + J\underline{p}_k + \underline{u}_k \tag{18}$$

where $\underline{x}_k = \underline{x}(k\Delta t)$, $\underline{p}_k = \underline{p}(k\Delta t)$ and $\underline{y}_k = \underline{y}(k\Delta t)$, $k = 1,\cdots,N_s$, are the digitized state, load and output vectors, $A = e^{A_c\Delta t}$ is the state transition matrix for the discrete formulation, $B = (A - I)A_c^{-1}B_c$, $G = G_c$ and $J = J_c$.

The discrete-time state space equations (17) and (18) have been supplemented with the random vectors $\underline{w}_k$ and $\underline{\upsilon}_k$ to account for the stochastic system and measurement noise, respectively. It is assumed that $\underline{w}_k$ and $\underline{\upsilon}_k$ are mutually uncorrelated, zero mean, white noise processes with known covariance matrices $Q = E[\underline{w}_k \underline{w}_k^T]$ and $R = E[\underline{u}_k \underline{u}_k^T]$.

3.3 *Joint Input-State Estimation Technique*

Let $\hat{x}_{k|l}$ be the estimate of the state x_k given the load $\{d_n\}_{n=0}^{l}$ and let $P_{k|l} = E[(x_k - \hat{x}_{k|l})(x_k - \hat{x}_{k|l})^T]$ be the error covariance matrix. Based on the filter proposed in Lourens et al (2012b), the force and the state estimates are computed recursively in three steps: the input estimation

$$\begin{aligned} \tilde{R}_k &= GP_{k|k-1}G^T + R \\ M_k &= (J^T\tilde{R}_k^{-1}J)^{-1}J^T\tilde{R}_k^{-1} \\ \hat{p}_{k|k} &= M_k(d_k - G\hat{x}_{k|k-1}) \end{aligned} \tag{19}$$

the measurement update

$$\begin{aligned} L_k &= P_{k|k-1}G^T\tilde{R}_k^{-1} \\ \hat{x}_{k|k} &= \hat{x}_{k|k-1} + L_k(d_k - G\hat{x}_{k|k-1} - Jp_{k|k}) \\ P_{k|k} &= P_{k|k-1} - L_k(\tilde{R}_k - JP_{p[k|k]}J^T)L_k^T \\ P_{xp[k|k]} &= P_{xp[k|k]}^T = -L_k JP_{p[k|k]} \end{aligned} \tag{20}$$

and the time update

$$x_{k+1|k} = A\hat{x}_{k|k} + \hat{p}_{k|k}$$

$$P_{k+!|k} = [A\ B]\begin{bmatrix} P_{k|k} & P_{xp[k|k]} \\ P_{px[k|k]} & P_{p[k|k]} \end{bmatrix}\begin{bmatrix} A^T \\ B^T \end{bmatrix} + Q \tag{21}$$

The initial unbiased state estimate $\hat{x}_{0|-1}$ and its error covariance matrix $P_{0|-1}$ are assumed known.

In structural dynamics applications, numerical instabilities may arise when the number of contributing structural modes is less than the number of sensors or the number of loads applied to the structure. These instabilities are due to numerical deficiencies of the inverse of the matrices $\tilde{R}_k$, $J^T\tilde{R}_k^{-1}J$ and $JP_{p[k|k]}J^T$. To avoid these numerical deficiencies, the inverses of the aforementioned matrices are computed by truncating the expansion obtained by a singular value decomposition, keeping only the terms associated with the dominant singular values. The proposed technique is shown to avoid the numerical rank deficiency of the aforementioned matrices. For more details the reader is referred to the work by Lourens et al. (2012b).

It was demonstrated in Lourens et al. (2012b) that the best estimates are obtained by assuming the location of the forces to be unknown. This is a realistic situation encountered in all practical applications with operational vibrations. The forces are spatially distributed over the boundary of the structure. However, using the fact that there is a correlation between the spatially distributed forces, one can replace the forces by a number of independent forces acting on the structure. In the joint input-state estimation algorithm, a set of equivalent forces is thus assumed to act at a number of arbitrarily chosen locations. These locations are chosen in this study to correspond to the locations of the measurements used in the filter for the estimation. In this case, the filter was demonstrated to provide improved estimates of the states. It should be noted that the estimates of the equivalent forces do not correspond to any estimates of the unknown input forces.

The filter was shown to be very accurate in estimating the acceleration time histories at unmeasured locations in a structure using a limited number of measured acceleration time histories. For displacement and strain estimates, a low frequency drift was observed which deteriorates significantly the estimates of the displacement and strain time histories. To correct this behavior, the estimated modal displacement time histories are windowed in the time domain and then passed through a high pass filter to remove the low frequency components in the signal that causes the drift. The low cut-off frequency is chosen to be a fraction of the modal frequency value of the lowest contributing mode of the structure. These windowed and filtered modal displacements are then used to compute the displacement or strain time histories. It will be demonstrated in the application section that this filtering technique is very effective in correcting the estimates provided by the filter, yielding accurate estimates of the strain response time histories. The stress estimates at a location are then readily obtained from the strains using the linear constitutive relationships for the material.

4 APPLICATION

The proposed method for predicting the strain time history and fatigue accumulation is demonstrated using simulated and experimental data from a laboratory steel beam shown in Figure 1. The steel beam has an IPE100 cross section and a length of 3m. Plates of 150x150x15 mm are welded to its ends and it is suspended at both ends from a steel frame using flexible springs to simulate free-free boundary conditions. A series of accelerometers is placed along the beam to record its response to a force, applied at one of the free-free beam ends. The positions of the 19 acceleration sensors and the applied force are shown in Figure 1.

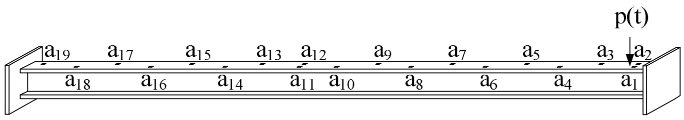

Figure 1: Laboratory steel beam model.

Modal tests were performed to identify the modal properties of the beam. Vertical accelerations on the top flange of the beam were measured at 17 different cross sections using 19 accelerometers. A force was repeatedly applied eccentrically using an impact hammer at one of the free-free beam ends.

The modal parameters of the beam were identified using the reference-based data-driven combined deterministic-stochastic subspace identification algorithm (Reynders and De Roeck 2008). The identified modal parameters were used to tune the Young's modulus of the steel and the stiffness of the springs in a FE model. More details on the tests, the results, and a comparison between the identified and computed eigenmodes can be found in Lourens et al. (2012a). Except for the torsional modes, whose contribution to the acceleration response considered is almost negligible, a good correspondence is found between the measured and experimental eigenfrequencies for up to 900 Hz. All modes are very lowly damped with damping ratios below 0.5%.

4.1 *Validation using simulated data*

A reduced-order state-space model is constructed from the eigenparameters of the updated FE model. The first 29 modes are included in the model, where f_{29} = 1006 Hz. Modal damping is set to 1%.

Simulated data are generated for two excitation cases applied eccentrically at one of the free-free beam ends: an impulse and a broadband stochastic excitation. The sampling frequency is set to 2000 Hz, and a period of 2 sec is analyzed, with the impulse applied at t = 0.5s. Ten accelerations are simulated, namely a1, a3, a4, a6, a9, a11, a15, a17, a18 and a19 (see Figure 1). Noise is added according to

$$\underline{\tilde{y}} = \underline{y} + g s \underline{r} \tag{21}$$

where $\underline{\tilde{y}}$ and $\underline{y}$ represent, respectively, the polluted and unpolluted time histories, g is the noise level, s signifies the standard deviation of the considered data time history, and $\underline{r} \in \mathbb{R}^N$ is a vector of random values drawn independently from a normal distribution with zero mean and unit standard deviation. The noise level g is set to 20 %.

The joint input-state estimation algorithm is used to identify the modal states and a set of equivalent forces, where the equivalent forces are assumed to act at the 10 data locations. Based on the order of magnitude of the state and data vectors the covariance matrices Q, R, and $P_{0|-1}$ are assigned values of 1e−8, 1e−2 and 1e−8, respectively, for the impulse excitation and 1e−6, 1e−2 and 1e−6, respectively, for the stochastic excitation.

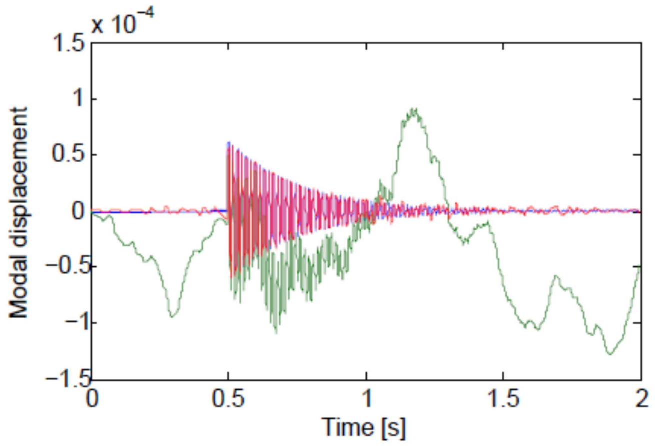

Figure 2: True (blue), identified (green) and filtered (red) modal displacement for f = 61 Hz and impulse excitation.

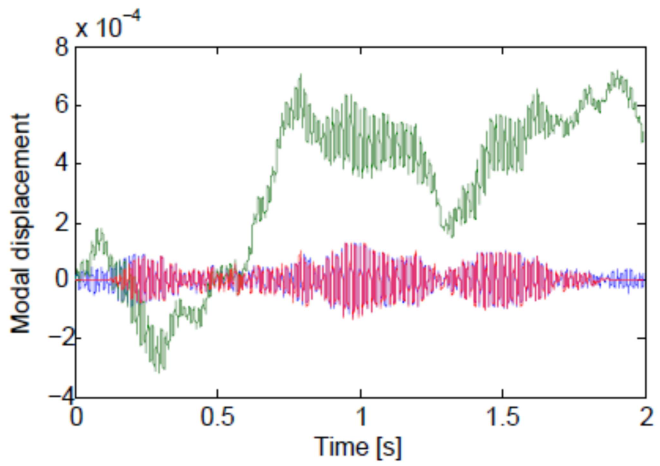

Figure 3: True (blue), identified (green) and filtered (red) modal displacement for f = 61 Hz and stochastic excitation.

The estimated modal displacements are first windowed and subsequently filtered using a 3rd order Chebyshev high-pass filter with a cutoff frequency of 0.3 times the values of the modal frequency. Figures 2 and 3 shows the identified modal displacements for the first bending (61 Hz) mode for the impulse and stochastic excitation cases, respectively. The figure shows the 1) true, 2) identified, and 3) windowed and filtered identified modal displacements. The low cut-off frequency in the high pass filter is chosen to be 0.3 times the modal frequency value of the lowest contributing mode of the structure.

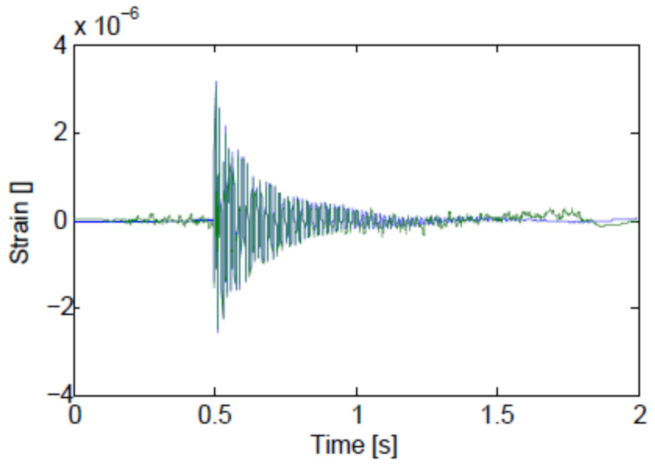

Figure 4: True (blue) and identified (green) strains at the middle top flange of the beam for the impulse excitation.

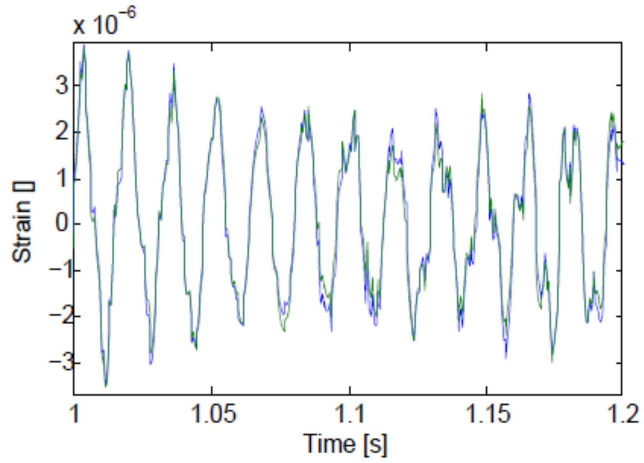

Figure 5: True (blue) and identified (green) strains at the middle top flange of the beam for the stochastic excitation.

It is obvious that the identified modal displacements contain a very low frequency drift which considerably deteriorates predictions of the displacement and strain response time histories. Such low frequency drift is not manifested in acceleration predictions, as was demonstrated in Lourens et al. (2012b). The use of the window and the filter corrects the identified modal displacements as shown in Figures 2 and 3. The identified (windowed and filtered) modal displacements are used to calculate the strain in the middle of the top flange at $L/2$, with L the length of the beam. These identified strains are compared to the true strains (calculated using the excitation and the updated model) in Figures 4 and 5 for the impulse and stochastic excitation cases, respectively. For the stochastic excitation, only 0.2s of the period is shown in the time-domain to make the results more visible. The fatigue damage accumulation results are compared in Table 1 using the identified and the true strain time histories. An extremely good prediction is noted which validates the effectiveness of the proposed methodology.

Table 1. Fatigue damage accumulation.

Fatigue	Validation using Simulated Data	
	Impulse Excitation	Stochastic Excitation
True	$1.19x10^{-9}$	$2.00x10^{-9}$
Identified	$1.20x10^{-9}$	$2.10x10^{-9}$

5 CONCLUSIONS

A methodology is presented for estimating damage due to fatigue on the entire body of a structure by combining linear damage accumulation laws, S-N fatigue curves, rainflow cycle-counting algorithms, and output-only vibration measurements at a limited number of locations. Using the available response time history measurements and a model of the structure, a joint input-state estimation filter and appropriate filtering techniques for the estimated modal displacement are used to estimate the strain response time histories. These strain response time histories are used to construct fatigue damage accumulation and lifetime prediction maps consistent with measurements provided by a monitoring system. Simulated measurements from laboratory steel beam model successfully validated the effectiveness and accuracy of the methodology. No assumptions were made about the temporal and spatial variation of the loads applied on the structure.

The proposed method of monitoring/mapping the fatigue damage accumulation in the hot spot locations of a structure is an invaluable tool for designing optimal fatigue-based maintenance strategies for most critical components of metallic structures using actual structural vibration information collected from a sensor network. Such techniques will be important in a number of applications, including prediction of fatigue in railway/motorway steel bridges, steel frame buildings and towers, turbines blades and towers, offshore structures, etc.

REFERENCES

American Society for Testing and Materials. 1997. Standard Practices for cycle counting in fatigue analysis.

Ching, J., Beck, J.L. &Porter, K.A. 2006. Bayesian state and parameter estimation if uncertain dynamical systems. *Probabilistic Engineering Mechanics* 21: 81-96.

Chatzi, E.N. & Smyth, A.W. 2009. The unscented Kalman filter and particle filter methods for nonlinear structural system identification with non-collocated heterogeneous sensing. *Structural Control and Health Monitoring* 16: 99–123.

EN 1993-1-9 Eurocode 3. Design of steel structures - part 1-9: fatigue. CEN. 2005.

Gillijns, S. & De Moor, B. 2007. Unbiased minimum-variance input and state estimation for linear discrete-time systems. *Automatica* 43(1): 111–116.

Gillijns, S. and De Moor, B. 2007. Unbiased minimum-variance input and state estimation for linear discrete-time systems with direct feedthrough. *Automatica* 43(5): 934–937.

Hernandez, E.M. and Bernal, D. 2008. State estimation in structural systems with model uncertainties. *ASCE Journal of Engineering Mechanics* 134(3): 252–257.

Lourens, E., Reynders, E., De Roeck, G., Degrande, G. & Lombaert, G. 2012a. An augmented Kalman filter for force identification in structural dynamics. *Mechanical Systems and Signal Processing* 27(1): 446-460.

Lourens, E., Papadimitriou, C., Gillijns, S., Reynders, E., De Roeck, G. & Lombaert, G., 2012b. Joint input-response estimation for structural systems based on reduced-order models and vibration data from a limited number of sensors. *Mechanical Systems and Signal Processing* doi:10.1016/j.ymssp.2012.01.011.

Lutes, L.D. & Larsen, C.E. 1990. Improved spectral method for variable amplitude fatigue prediction. *Journal of Structural Engineering (ASCE)* 116(4): 1149-1164.

Miner M.A. 1945. Cumulative damage in fatigue. *Applied Mechanics Transactions (ASME)* 12(3): A159-A164.

Mottershead, J..E. & Friswell, M.I. 1993. Model updating in structural dynamics: A survey. *Journal of Sound and Vibration* 167: 347-375.

Ntotsios, E., Papadimitriou, C., Panetsos, P., Karaiskos, G., Perros, K. & Perdikaris, P. C. (2009). Bridge Health Monitoring System based on Vibration Measurements. *Bulletin of Earthquake Engineering* 7 (2): 469-483.

Palmgren, A. 1924. Die Lebensdauer von Kugallagern. *VDI-Zeitschrift* 68(14): 339-341.

Papadimitriou, C., Beck, J.L. & Katafygiotis, L.S. 2001. Updating robust reliability using structural test data. *Probabilistic Engineering Mechanics* 16: 103-113.

Papadimitriou, C., Fritzen, C.-P., Kraemer, P. & Ntotsios, E., 2011. Fatigue predictions in entire body of metallic structures from a limited number of vibration measurements using Kalman filtering. *Structural Control and Health Monitoring* 18: 554-573.

Reynders, E. & De Roeck, G. 2008. Reference-based combined deterministic-stochastic subspace identification for experimental and operational modal analysis. *Mechanical Systems and Signal Processing*, 22(3): 617–637.

Teughels, A. & De Roeck, G. 2005. Damage detection and parameter identification by finite element model updating." *Archives of Computational Methods in Engineering* 12(2): 123-164.

Tunna, J.M. 1986. Fatigue life prediction for gaussian random loads at the design stage. *Fatigue and Fracture of Engineering Materials and Structures* 9: 169–184.

Wu, M. & Smyth, A.W. 2007. Application of the unscented Kalman filter for real-time nonlinear structural system identification. *Structural Control and Health Monitoring* 14: 971–990.